16TH EUROPEAN CONFERENCE ON EARTHQUAKE ENGINEERING THESSALONIKI 18 - 21 JUNE 2018

IN-PLANE RESPONSE AND DAMAGE ASSESSMENT OF HOLLOW CLAY INFILL PANELS IN RC BUILDINGS

Maria Teresa DE RISI[1], Carlo DEL GAUDIO[2],
Paolo RICCI[3], Gerardo Mario VERDERAME[4], Gaetano MANFREDI[5]

ABSTRACT

Reinforced Concrete (RC) framed buildings with clay masonry infills represent a very common structural typology worldwide for civil, strategic or productive use. Nevertheless damage to infills may cause danger for human lives and strongly affected economic losses due to past earthquakes, in current practice, infills are considered as partition elements without any structural function. However, their role is crucial in terms of global and local response of RC buildings in the event of earthquake. Their behaviour under seismic actions should be reliably characterized, starting from the analysis of their displacement capacity at different performance levels due to in-plane actions, and a proper numerical modelling, able to reproduce the influence of infills on the global behavior of RC frames under seismic actions. Some models have been already proposed in literature, but their reliability should be yet proved on the basis of an as huge as possible experimental database.
In this paper, a homogenous extensive database of experimental tests on RC frames infilled with hollow clay-masonry infills – typical of Mediterranean RC building stock – is collected and presented. The experimental responses of masonry infills under lateral loads are obtained. The main numerical models existing in literature for infills are investigated and compared with the experimental results in order to select the model that minimize the prediction error or to propose a new simplified model for the envelope of the infill response.
The evolutions of damage under increasing displacement demand are also analyzed, and the displacement capacity at given performance levels are identified and correlated to the in-plane response of the infill panels. The analysis of the damage evolution to the infills during the experimental tests finally allows the definition of drift-based fragility functions for these non-structural components, representing a key point for a reliable estimation of losses due to earthquakes.

Keywords: RC buildings; masonry infills; experimental database; numerical modelling; drift-based fragility curves.

1. INTRODUCTION

Earthquakes occurred in last twenty years in Italy had a significant impact at economic and social level. Damage to non-structural components, namely, infills and partitions, in Reinforced Concrete (RC) Moment Resisting Frames – a very widespread constructive solutions for RC structures for civil or productive aims – often played a key role. Nevertheless, infill panels are generally neglected in practice-oriented structural analyses for design or assessment purposes. On the contrary, the seismic

---

[1]Postdoctoral Research Fellow, University of Naples Federico II Department of Structures for Engineering and Architecture, Naples, Italy, beneficiary of a AXA Research Fund postdoctoral grant, mariateresa.derisi@unina.it
[2]Postdoctoral Research Fellow, University of Naples Federico II Department of Structures for Engineering and Architecture, Naples, Italy, carlo.delgaudio@unina.it
[3]Assistant Professor, University of Naples Federico II Department of Structures for Engineering and Architecture, Naples, Italy, paolo.ricci@unina.it
[4]Associate Professor, University of Naples Federico II Department of Structures for Engineering and Architecture, Naples, Italy, verderam@unina.it
[5]Full Professor, University of Naples Federico II Department of Structures for Engineering and Architecture, Naples, Italy, gamanfre@unina.it

behaviour of masonry infills should be reliably characterized aiming at a correct definition of fragility functions for this structural typology. Therefore, a proper nonlinear modelling is necessary to reproduce the influence of infills on the global behaviour of RC frames under seismic actions from the onset of damage to collapse, and the analysis of their displacement capacity at different performance levels (PLs) or Damage States (DSs) is required to improve the damage assessment and loss evaluation due to earthquakes.
Some experimental and analytical investigations were performed on infilled RC structures in last decades, about the influence of infills on local and global seismic performance of structures. Unfortunately, experimental data used to calibrate or validate these models are always quite limited or very heterogeneous, and therefore, their reliability should be proved and compared each other based on an as huge as possible homogeneous experimental database.
Furthermore, in last years, several studies (e.g. Colangelo, 2013; Cardone and Perrone, 2015; Sassun et al., 2016; Chiozzi and Miranda, 2017) have been focused on the definition of displacement thresholds corresponding to given physical damage levels on infill partitions and on the uncertainty related to their assessment. In some cases, drift-based fragility functions were also carried out for each DS, considering together experimental data related to different frame typologies (RC or steel), brick typologies (solid clay; hollow clay; concrete units), and configurations (solid panels or panels with openings).
In this paper, a homogenous extensive database of experimental tests on RC frames infilled with hollow clay-masonry bricks – typical of Italian and Mediterranean RC building stock – is collected and presented. This database represents a huge collection of data referred to the specific brick typology herein investigated. Starting from the collected data, the experimental response of masonry infills under lateral loads are obtained by means of the experimental responses of the infilled frames and the corresponding bare frames. The main and widely used numerical models existing in literature for infills are investigated and compared with the experimental results. In particular, such an analysis is performed in the context of single-strut models, able to well reproduce the influence of the infill panel on the global response of the infilled frame (Ricci et al., 2013). Predicted-to-experimental ratios related to the main parameters that describe the envelope of the infill response are obtained and analysed for models proposed by Bertoldi et al. (1993) and Panagiotakos and Fardis (1996). Finally, a modification of the latter model is proposed to obtain a simple practice-oriented force-displacement envelope to significantly reduce the mean percentage errors in the prediction of the infill in-plane behaviour under lateral loads.
Thanks to the analysis of the evolutions of damage under increasing displacement demand for the collected tests, the displacement capacity at given performance levels are also identified and correlated to the previously defined in-plane behaviour of the infill panels. Empirical cumulative distribution functions are then evaluated for four different DSs, and lognormal fragility functions are used to fit such data by means of the Method of Maximum Likelihood. The influence of openings on the displacement capacity of infills with hollow clay bricks is also investigated.

2. EXTPERIMENTAL DATABASE

The first step of the present research is the collection of a comprehensive database of tests on infilled RC frames. More than 200 experimental tests performed and presented in literature during last four decades have been analysed and divided in homogeneous subsets depending on the infill and frame typology. In particular, only tests characterized by unreinforced masonry (URM) with hollow clay (HC) bricks are considered herein, being one of the most widespread partition typology used in RC moment resisting frames of Mediterranean building stock.
Starting from the whole database, 105 one-bay-one-storey tests with RC frames and, in particular, first, tests without openings (89) have been selected. Sixty of these tests were completely described by the Authors of the experimental campaigns, including the description of the infill panel damage evolution, but only in 38(/60) cases, the experimental response related to the corresponding bare frame was also explicitly presented by the Authors. Therefore, starting from the 89 tests about infill panels without openings, only 60 are useful for the purposes of this study. In particular:

- 39(/60) tests are characterized by a description of the infill damage depending on the imposed lateral displacement, which can be associated with the DSs defined and adopted herein;

•	for 38(/60) tests, it was possible to evaluate the experimental response of the infill panel, since it was provided by the Authors or explicitly calculated as the difference between the response of the infilled RC frame and the corresponding bare frame (as explain later in Section 3); 17 of these 38 tests are also characterized by the complete description of the damage evolution to the infill panel.

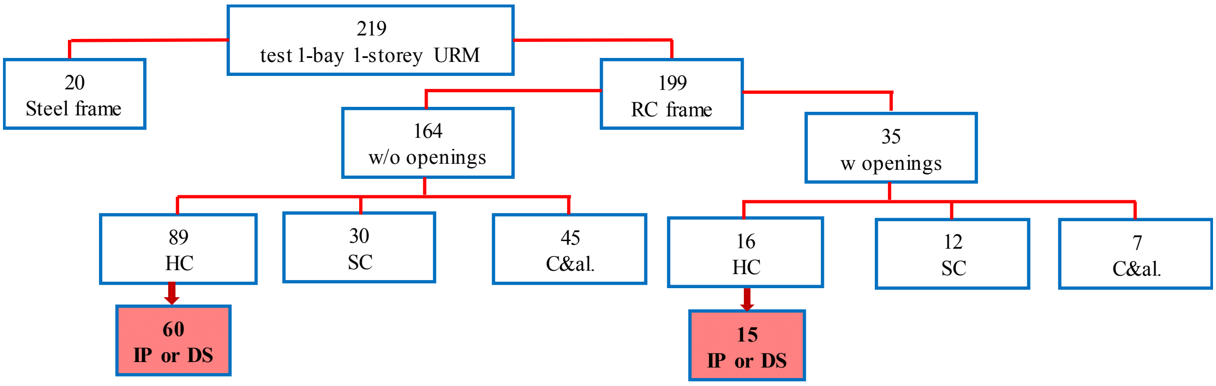

Figure 1. Collected database from literature (URM = Unreinforced masonry infills; HC = hollow clay bricks; SC = solid clay bricks; C&al. = concrete blocks or other material; DS = description of Damage State evolution available; IP = In-Plane response available (i.e. corresponding experimental bare frame available)

In summary, 90% of the collected solid infill panels are characterized by an aspect ratio (H_w/L_w) $\leq$1.00; 80% of the specimens are characterized by a slenderness ratio (H_w/t_w) $\leq$15. Approximately 90% of infill panels is constituted by hollow clay bricks with a void percentage at least equal to 45%. The 60% of the infills is characterized by bricks with horizontal orientation of the holes. More details about the collected tests can be found in De Risi et al. (2017, 2018) and Del Gaudio et al. (2017, 2018).
Additionally, a database of only 15 tests useful for the purpose of this study and specific on hollow clay brick infilled frames with openings (doors or windows) can be found from literature (see Figure 1). Scaled tests both with doors and windows are considered, characterized by opening percentages ranging between 10% and 40%, brick void percentage between 36% and 60%, and infill slenderness ratio (H_w/t_w) between 10.8 and 13.3.

3. IN-PLANE BEAHVIOUR

In this Section, the attention is focused on the in-plane lateral load-displacement response of the investigated typology of infill panels. The experimental response of infills are first obtained and analysed as explained in Section 3.1, starting from a subset of tests belonging to the collected database. Then, the prediction capability of two main macro-models adopted in literature is investigated (Section 3.2) in the context of the single-equivalent-strut modelling approach. Finally, a comparison between numerical modelling proposals from literature and collected experimental data is carried out, and a simple modification of an existing model is proposed, to significantly reduce the mean prediction errors of the infill in-plane behaviour (Section 3.2).

3.1 Experimental response of the infill panels

The experimental responses of each infilled frame and each corresponding bare frame have been first digitalised for all the tests belonging to the database. Then, the first-cycle envelopes of such responses have been obtained. Finally, the infill experimental response of each test – in terms of horizontal load (F)-versus-horizontal displacement (D) – has been derived as the difference between the infilled frame and the corresponding bare one, assuming that the RC frame and the infill panel work as a parallel system (i.e. under equal displacement). The described procedure implies that the RC surrounding frame will exhibit the same base shear-top displacement response in bare and infilled configurations. Such a hypothesis is not completely rigorous, but often suggested and adopted in literature (e.g. Fardis, 1997; Hak et al., 2013; Bergami and Nuti, 2015) to obtain the infill lateral response. Since all the tests are cyclic tests and all the specimens are symmetric, each force-displacement response has been finally averaged between positive and negative loading direction. Note that the procedure described above requires the knowledge of the experimental response of both the infilled frame and the corresponding bare frame. "Hybrid experimental responses" could be derived by means of numerical simulations of the bare frames, when their experimental responses are missing. Nevertheless, such hybrid responses implicitly contain also the error deriving from the modelling of the bare frame, and therefore, in this work they are not considered. As a result, 38 of the 60 collected tests (see Section 2) have been adopted to analyse the in-plane response of the investigated infill typology.

The analysed experimental responses generally clearly show a high initial stiffness until first cracking occurrence and a subsequent stiffness degradation up to the peak load. After maximum lateral load is reached, a degrading branch can be easily recognised. Therefore, for all the experimental responses some characteristic parameters have been recognised (Figure 1a), namely: peak load (F_{peak}); cracking strength (F_{cr}); secant-to-cracking stiffness (K_{cr}); secant-to-maximum stiffness (K_{peak}); softening stiffness (K_{soft}). Figure 1b shows the result of the multi-linearization of the experimental responses for all the tests here investigated, defined on the basis of three main characteristic points: cracking point ($F=F_{cr}$), peak load ($F=F_{peak}$) and softening linear branch (characterized by a negative slope equal to K_{soft}).

Note that the peak point is generally clearly identified on the experimental envelope. On the other hand, the cracking point has been detected starting from the observation of damage evolution and the analysis of the lateral force-displacement response for each test: the first observed macro-cracking of the panel produces a first significant change in tangent stiffness of the experimental force-displacement envelope. Note also that the cracking point identifies a secant stiffness on each envelope (K_{cr}) that is lower than the initial elastic stiffness characterizing the response until the very first detachment of the infill panel from the surrounding frame is observed. Such an elastic stiffness is generally not evaluable in a reliable way due to the bad quality of some experimental responses in their very initial stage of behaviour. However, cracking-to-peak strength ratio is, on average, equal to about 0.67. This result is in tune with main modelling proposals from literature, such as models by Bertoldi et al. (1993), Panagiotakos and Fardis (1996) or proposal by Dolsek and Fajfar (2008) – which suggest a cracking-to-peak strength ratio equal to 0.80 (De Sortis et al., 2007), 1/1.30 and 0.60, respectively. Softening and cracking stiffness appear as the most challenging parameters, due to their high variability among the collected tests. Ratios K_{soft}/K_{peak} and K_{cr}/K_{peak} show a coefficient of variation (CoV) equal to 64% and 73%, respectively (see De Risi et al., 2017; 2018).

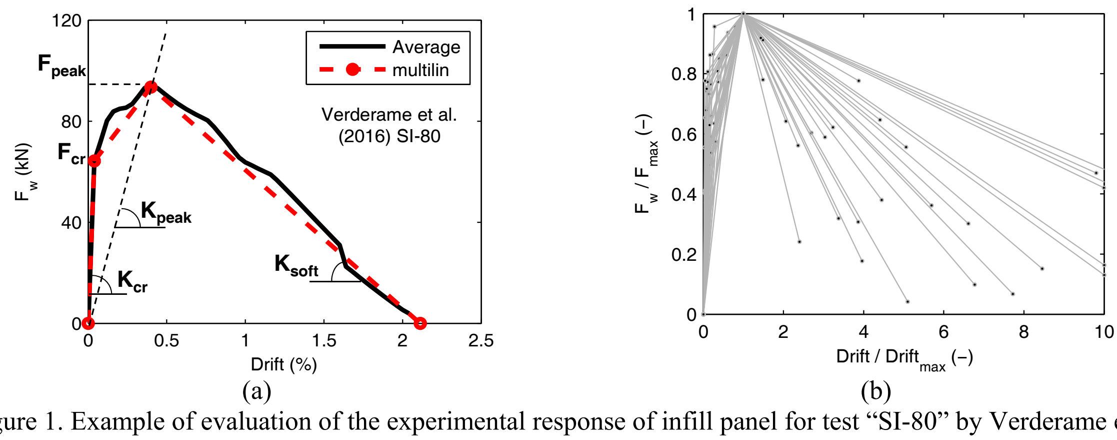

Figure 1. Example of evaluation of the experimental response of infill panel for test "SI-80" by Verderame et al. (2016) - analysed parameters (a); multi-linearized experimental responses of the investigated infills (b).

3.2 Numerical versus experimental comparisons

The experimental envelopes - obtained as explained in the previous Section - are compared herein with two different infill models existing in literature, which define a complete lateral force-displacement response, and have been often adopted in numerical analyses in last years, namely models by Bertoldi et al. (1993) and Panagiotakos and Fardis (1996).

The first model considered herein to define the envelope curve of the force-displacement relationship for the equivalent strut is the model proposed by Bertoldi et al. (1993) ("B. et al." in the following).

Such a model is the only one among those considered herein that is able to account for and predict the failure mode that can be exhibited by the infill panel. It was proposed and validated on the basis of experimental results mostly including tests on structural-masonry walls. According to Bertoldi et al. (1993), the envelope of the hysteretic response of infilled frames under lateral loads is characterized by *(a)* a first detachment between the infill and the surrounding frame, followed by *(b)* the complete cracking of the infill panel, and *(c)* the achievement of a maximum lateral load, starting from which *(d)* a degrading phase begins. Model by Bertoldi et al. (1993) proposes a simplification of such a behaviour by means of a quadri-linear backbone as shown in Figure 2a, where:

- F_{max} depends on the predicted failure mode depending on the infill mechanical properties, such as: cracking shear strength (τ_{cr}) obtained by diagonal compression tests, sliding strength of the bed joints (u) derived from "triplet tests", compressive strength of masonry (f_m) and vertical stress (σ_0) acting on the infill;
- K_{sec} depends on mechanical and geometrical parameters, such as the equivalent strut width, defined by means of the parameter (λ_h) by Stafford and Smith (1963) and suggestions by Bertoldi et al. (1993) about the strut width;
- cracking-to-peak and residual-to-peak strength ratios, cracking-to-peak and softening-to-peak stiffness ratios are defined according to De Sortis et al. (2007).

Model by Panagiotakos and Fardis (1996) ("P&F" in the following) has been calibrated on the basis of ten tests on infilled RC frames with hollow bricks masonry and horizontal holes by Pires and Carvalho (1994) and Stylianidis (1984) that mainly exhibited a diagonal cracking failure mode. Also, this envelope is made up of four branches (see Figure 2b). The first branch of such a model corresponds to the linear elastic behaviour up to cracking. The second branch continues up to the maximum strength F_{max}, mainly depending on the cracking shear strength and the horizontal area of the infill panel. The secant-to-peak stiffness corresponds to the Mainstone's (1971) stiffness (K_{MS}). The third branch of the envelope is a degrading branch up to the achievement of a residual strength; its slope (K_{deg}) depends on the elastic stiffness through the parameter (α), fixed by the Authors (Panagiotakos and Fardis, 1996) within the range of values 0.5-10%. Last branch is horizontal; it corresponds to a residual constant strength; residual-to-maximum strength ratio (β) can be assumed equal to 1-2% (Panagiotakos and Fardis, 1996). In the following, the ratio between post-capping degrading stiffness and elastic stiffness is assumed equal to α=0.03, and the residual-to-maximum strength ratio is assumed equal to β=0.01.

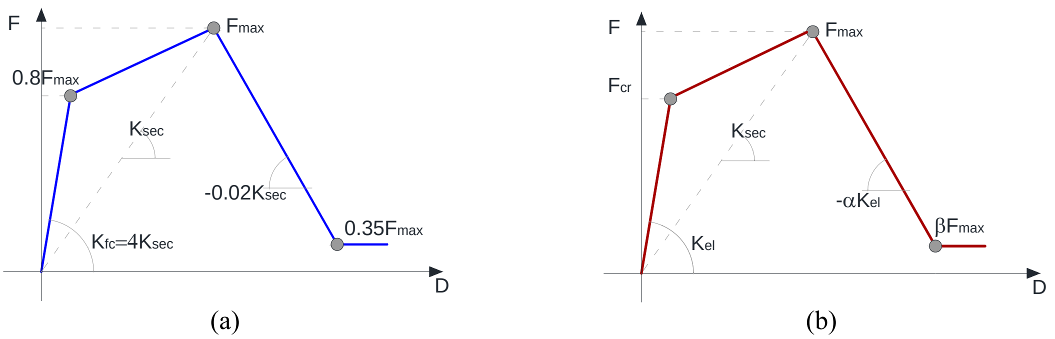

Figure 2. Force-displacement envelopes for infills according to models by Bertoldi et al. (1993) (a) and Panagiotakos and Fardis (1996) (b)

The applicability of both these models requires the knowledge of the mechanical properties mentioned above. In particular, shear cracking strength (τ_{cr}), Young modulus (E_w) and shear modulus (G_w) of masonry are required to apply the model by Panagiotakos and Fardis (1996), whereas more mechanical properties have to be known if model by Bertoldi et al. (1993) has to be applied. Generally mechanical properties have been obtained by the test report of the experimental campaigns carried out by the Authors. Otherwise, in the absence of data explicitly reported by the Authors, some assumptions have been taken. In particular, the Young's modulus of the masonry (E_w) is a function of the comprehensive strength of a masonry prism (f_{me}), as suggested by FEMA 306. Also sliding strength of the bed joints (u) is evaluated according to the formulation suggested by FEMA 306 for the cohesive capacity of the mortar beds. The expected shear modulus of masonry, (G_w) is taken as 0.40 times the Young's modulus of the masonry (E_w), as suggested by FEMA 356 for masonry and commonly adopted in literature. Finally, shear strength (τ_{cr}) is calculated as 0.275 times the square root of the comprehensive strength of a masonry prism (f_{me}), as suggested and applied in Jeon et al. (2015) on the basis of experimental studies performed by Drysdale (1984). Note that also other formulations are reported in literature to predict the shear cracking strength of masonry, such as proposals by FEMA 306; nevertheless, predicted values by Jeon et al. (2015) appears the closest to experimental values, whereas a significant underestimations of shear cracking strength is observed if proposal by FEMA 306 is applied.

The infill models previously described have been applied to the collected tests. Errors in terms of strength and stiffness corresponding to main characteristic points of the infill response have been evaluated. Mean values of the relative percentage errors (e_r) (Eq. 1) are shown in Table 1 together with their coefficients of variation for both the investigated models.

$$e_r = \frac{(\text{pred}) - (\text{exp})}{(\text{exp})} \cdot 100 \qquad (1)$$

It can be observed that the model by "B. et al" significantly underestimates peak strength and cracking strength (of about -60% and -44%, respectively) (see Table 1). Such a result can be ascribable to the failure mode (FM) prediction according to this model. As a matter of fact, about 68% of tests are classified as "Sliding Shear" FM, providing a maximum strength that is the lowest among the possible FMs and, in particular, generally lower than the corresponding experimental value. The error in terms of FM prediction for model by "B. et al." has been also evaluated: only in the 30% of cases the model is able to well predict the observed FM. On the other hand, the model by "P&F" overestimates peak load of about +35% and cracking strength of +83% (Table 1).

Cracking and peak stiffness are overestimated by both the models (Table 1). In particular, model by "B. et al" provides mean relative percentage errors equal to about 260% both for K_{cr} and K_{peak}. Model by "P&F" overestimates cracking stiffness of about 88% and secant-to-peak stiffness of about 27%. Therefore, secant-to-peak stiffness assessed according to Mainstone (1971) – and assumed by "P&F" model – shows, on average, the lowest error, even if with a consistent dispersion in the prediction. On the other hand, cracking stiffness by "P&F" model theoretically corresponds to a pure shear elastic behaviour of the panel and, therefore its underestimation with respect to an experimental macro-cracking stiffness is expected.

The error in terms of K_{soft} is also computed (Table 1) depending on the assumptions explained above about the assessment of this parameter (α = 3% for model by "P&F" and K_{soft} = -2% K_{peak} for model by "B et al."). It should be noted that Panagiotakos and Fardis (1996) proposed a very wide range of values for K_{soft} covering two orders of magnitude, but a single value as been chosen herein for sake of comparison. As a result, model by "P&F" overestimates the softening stiffness with respect to the experimental values (e_r is equal to about +75%), whereas model by "B. et al." underestimates such a stiffness of 47%. In both cases coefficients of variation have quite high values. CoV are always higher than 50% (see Table 1) for all the investigated parameters, and, generally, a bit lower if the model by P&F is considered.

Table 1. Summary of relative percentage errors and CoV for the investigated infill models

	P&F		**B et al.**		**B et al. – observed FM**	
	e_r (%)	**CoV** (%)	**e_r** (%)	**CoV** (%)	**e_r** (%)	**CoV** (%)
F_{cr}	83	89	-44	97	80	244
K_{cr}	88	72	260	87	260	87
F_{peak}	35	58	-60	68	5	146
K_{peak}	27	83	266	73	266	73
K_{soft}	75	76	-47	62	-47	62

It was observed that the model by "B et al." is able to take into account the failure mode of the infill

panel, but the predicted FM is generally not coincident with the observed FM for the tests belonging to the collected database (De Risi et al., 2017, 2018). Nevertheless, it should be noted that, if peak load by "B et al." model is calculated by assuming the observed FM as an input data, the percentage error drastically reduces at F_{peak} (about +5%), even if with a very high coefficient of variation (146%) (see Table 1). Errors in terms of predicted stiffness remain unvaried. Unfortunately, such an application of this model is not possible when a-priori predictions are required.
Another analysis of the errors discussed above can be carried out if two distinct subsets of data are considered, namely if tests with horizontal holes bricks and tests with vertical holes bricks are considered separately (see Table 2). On average, infills with vertical holes have lower void percentage bricks, higher compressive (+155%) and shear (+115%) strength with respect to panels with horizontal holes – the latter generally exhibiting a diagonal cracking failure mode. It can be observed that the accuracy of the model by "B et al." does not change significantly, whereas the model by "P&F" significantly improves its prediction capability for infills with horizontal holes, especially at peak stiffness – mean e_r becomes about +3% – and peak load – mean e_r becomes equal to about +11% (with a CoV equal to 32%). Also error in terms of cracking load decreases to +33% with a lower CoV (from +89% to 46%) if only infills with horizontal holes are considered.

Table 2. Summary of relative percentage errors and CoV for the investigated infill models, considering two separated subset of data: horizontal holes and vertical holes

	Horizontal holes				**Vertical holes**			
	P&F		**B et al.**		**P&F**		**B et al.**	
	e_r (%)	**CoV** (%)	e_r (%)	**CoV** (%)	e_r (%)	**CoV** (%)	e_r (%)	**CoV** (%)
F_{cr}	33	46	-56	47	207	83	-13	105
K_{cr}	78	67	216	86	112	80	368	83
F_{peak}	11	32	-65	38	92	63	-49	89
K_{peak}	3	59	227	69	88	87	359	74
K_{soft}	122	67	-38	53	2	54	-61	77

Starting from previous remarks, the model by "P&F" generally shows CoV values that are lower than those related to the model by "B et al". Furthermore, model by "P&F" appears easier to apply since, it requires a very limited number of mechanical parameters to be defined, even if it is not able to predict a failure mode for the infill panel. Consequently, herein, finally a slight modification of the model by "P&F" is proposed, as shown in Figure 3 (hereinafter referred to as "ModP&F envelope"). In particular, starting from the analysis of the mean error related to the prediction of peak load by "P&F" model, it is assumed that F_{peak} is equal to the cracking strength predicted by the "P&F" model. The analysis of the experimental cracking-to-peak-load values suggests that such a ratio can be assumed equal to 0.7. Secant-to-peak stiffness predicted according to the Mainstone's proposal (K_{MS}) is corrected by a factor of 0.8. Secant-to-cracking stiffness and softening stiffness are finally prosed as a fraction of K_{MS}. In such a way, mean relative errors - obtained by comparing "ModP&F envelope" and experimental infill responses - result lower than 3% for all the parameters required to define the backbone curve. On the other hand, since the simplicity of this approach, CoV remain generally unvaried with respect to the application of "P&F" model (Table 3). Certainly further efforts should be performed in future works to investigate about this variability – starting from the variability of the experimental data – and reduce the dispersion in the prediction. Further studies should be performed to produce a more detailed analysis about the influence of mechanical and geometrical parameters on the key points of the nonlinear response, also taking into account a higher amount of proposals from literature, thus trying to reduce the currently high coefficient of variations in prediction capacity.

Table 3. Summary of relative percentage errors and CoV for the ModP&F envelope

ModP&F	F_{cr}	K_{cr}	F_{peak}	K_{peak}	K_{soft}
e_r (%)	0.96	-2.65	0.96	1.91	-0.97
CoV (%)	57	58	69	58	83

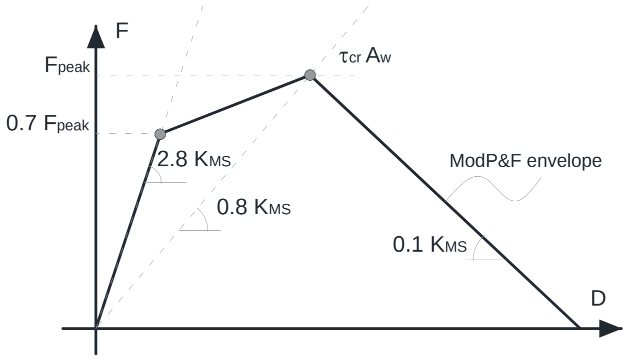

Figure 3. Proposed envelope ModP&F (Modified Panagiotakos and Fardis)

4. DAMAGE ASSESSMENT

Starting from the analysis of the evolutions of damage under increasing displacement demand for the collected tests, the displacement capacity at given performance levels have been also identified and correlated to the previously defined in-plane behaviour of the infill panels, as explained in this Section.

4.1 Definition of Damage States (DSs) and collected data

Several studies (Colangelo, 2013; Cardone and Perrone, 2015; Chiozzi and Miranda, 2017) have been focused on the definition of displacement thresholds corresponding to given physical damage levels on infill partitions and on the uncertainty related to their definition. Some authors define different DSs through the observation of extent and severity of cracking patterns observed on the panels or of the failure typology of brick units; some others, additionally, relate such damage levels to the attainment of the peak load of the infilled frame or to the achievement of given strength reduction ratios. Generally speaking, three or four DSs are defined in literature, corresponding, respectively, to: *(i)* the onset of cracking and first detachment between infill panel and surrounding RC frame; *(ii)* the widening of previous damage pattern; *(iii)* the crushing and spalling of a considerable number of brick units; *(iv)* the partial/total collapse of the infill panel.

In this study, the definition of Damage States (DSs) is assumed according to the proposal by Cardone and Perrone (2015). Such a definition is basically based on AeDES survey forms (Baggio et al., 2007), which are commonly adopted in the Italian framework to decide about the usability of buildings after earthquakes – also considering infills – to properly address consequently repair actions and funds for reconstruction. Furthermore, this definition of DSs appears more objective since it also clearly provides a quantitative information about the extension of the panel area affected by cracks or possible failure of brick units. Indeed DS1 *(Light Cracking)* and DS2 (*Extensive cracking*) are very similar to those defined in the AeDES form, reporting further indications about the width of diagonal cracks (1 mm<width<2 mm) and about the extension of the panel area affected both by cracks (25-35%) and by possible failure of some brick units (10%) for what concerns DS2. Furthermore, the Authors assume that DS3 *(Corner crushing)* corresponds to a wide spreading of crushing and spalling of brick units (to 30% of the panel area), and DS4 *(Collapse)* to the in-plane or out-of-plane (whichever occurs first) global collapse of the infill panel.

As a result of such a definition of damage states, when no openings are present in the infill panel, collected IDR values at DS1 show a quite high dispersion, ranging between 0.02% and 0.35% (CoV=0.81). DS2 and DS3 are achieved for IDR belonging to the ranges [0.12%; 0.70%] (with CoV = 0.40) and [0.40%; 1.75%] (with CoV=0.43), respectively. Finally, DS4 is reached for IDR varying between 0.94% and 3.25% (CoV=0.34). Lower variability is shown for tests with openings at DS1 and DS2 with respect to tests without openings, since IDR values range between 0.09% and 0.11% (CoV=0.08), and 0.18% and 0.39% (CoV=0.23), respectively. IDR values belong to the ranges [0.35%; 0.58%] (with CoV = 0.21) and [0.50%; 3.48%] (with CoV=0.47), at DS3 and DS4, respectively.

4.2 Drift-based fragility curves for solid panels

First data related to tests on infill without openings (namely solid panels) are investigated in this Section. For each DS, the empirical cumulative distribution (ECD) of IDR is obtained by plotting ascending-ordered drift ratio values against *(i-0.5)/n*, where "*i*" is the position of the drift ratio value in the ordered list of drift ratios and "*n*" is the total number of drift values for that damage state. The ordered data have been also revised to delete possible spurious values, which reflect experimental errors or misinterpretation of experimental results. To this end, the Peirce's criterion (Ross, 2003) has been applied, as suggested by FEMA-P58. Then, the Method of Maximum Likelihood has been used to fit ECDs with lognormal fragility function (LN_CDF), as usual in this kind of applications. The choice of LN_CDF is essentially due to its properties: firstly, x-axis is restricted to the interval (0, +∞), and secondly the distribution appears to be skewed to the left, reflecting the frequency of the observations of data gathered in the lower values of x-axis. As well known, a lognormal fragility function is fully defined by only two statistical parameters, as shown in Eq. (2).

$$\mathrm{LN\_CDF}\left(\mathrm{DS} \geq \mathrm{ds_i} | \mathrm{IDR_j}\right) = \Phi\left(\frac{\ln\left(\mathrm{IDR_j}\right) - \mu_i}{\beta_i}\right) \tag{2}$$

where $\mathrm{LN\_CDF}\left(\mathrm{DS} \geq \mathrm{ds_i} | \mathrm{IDR_j}\right)$ is the conditional probability that the component will experience or exceed the ith damage state given the inter-storey drift value, IDR_j; $\Phi\ (\cdot)$ is the standard normal cumulative distribution function; (μ_i) is the logarithmic mean value; (β_i) is the logarithmic standard deviation. The resulting LN_CDFs for the four DSs are shown in Figure 4.

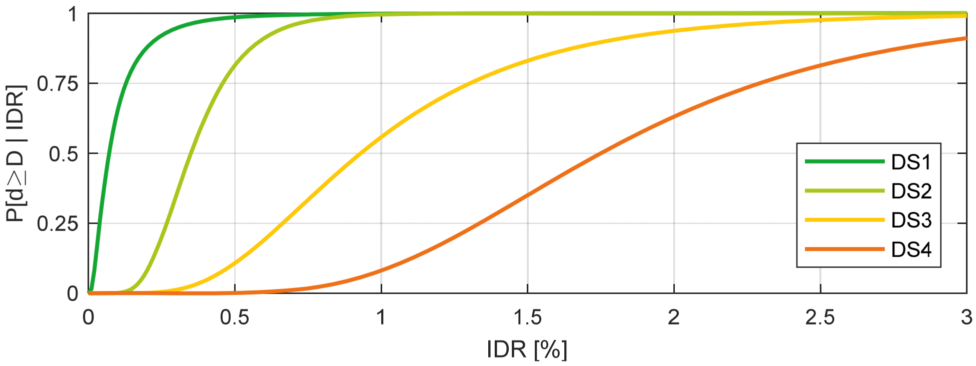

Figure 4. Proposed fragility function curves for hollow clay brick solid infill panels

Note that the total dispersion, β_i, represents the uncertainty in the actual value of IDR at which a damage state is likely to start. If fragility curves are obtained based on a limited set of experimental data, two sources of uncertainty should be considered. The first one ($\beta_{r,i}$) represents the random variability observed in the collected data from which the fragility parameters are calculated. The second source ($\beta_{u,i}$) represents uncertainty in the difference between testing specimens/procedures and actual installation/loading conditions, or uncertainty that the available data are an adequate sample size to accurately represent the true random variability (FEMA P-58). The total dispersion at the ith DS, (β_i), is finally computed as the square root of the sum of squares of $\beta_{r,i}$ and $\beta_{u,i}$, as shown in Eq. (3):

$$\beta_i = \sqrt{\beta_{r,i}^{\ 2} + \beta_{u,i}^{\ 2}} \tag{3}$$

The value of $\beta_{u,i}$ is assumed ranging between 0.10 and 0.40, mainly depending on the sample size of available data (FEMA-P58, Lowes, 2009). In summary, the resulting median drift capacity (e^{μ_i}) and the number of tests actually used for each DS (n_i, i=1,…,4) among the total number of tests (N=39) are reported in Table 4. Logarithmic standard deviations of LN_CDFs *(i)* that come from the available data ($\beta_{r,i}$), and *(ii)* obtained through Eq. (3) (approximated to the first decimal place) are also reported.

Table 4. Parameters related to the proposed fragility functions for hollow clay brick solid infill panels

DS	n_i	e^{μ} (%)	β_r	β
DS1	33	0.07	0.91	0.90
DS2	21	0.35	0.43	0.40
DS3	14	0.93	0.46	0.50
DS4	25	1.75	0.37	0.40

4.2.1 Relationship between in-plane response and damage assessment

The displacement capacity of infill panels has been investigated by means of "observational" data only for all DSs, without any consideration of the in-plane force -displacement response of the infill panel. However, it could be very interesting to find the relationship between the observed displacement capacity at each DS and the related drift at the peak load of the infill panel in-plane response (IDR_{peak}), to be used, for example, if it is necessary to derive information about DSs starting from the in-plane response of the panel only. Herein, such a correspondence is directly quantified on the basis of the experimental results, starting from the analysis of the response of the infill panel, obtained as explained in Section 3. In particular, for a subset of tests (17 tests) characterized by both the description of damage evolution to the infill panel and by the force-displacement envelope of the infill panel, a functional relationship between the IDR value related to the i^{th} purely observed DS (IDR_i) and IDR value corresponding to the peak load of the infill experimental response (IDR_{peak}) is evaluated, as shown in Eq. (4):

$$IDR_i = \alpha_i \cdot IDR_{peak} \tag{4}$$

In particular, *Light Damage* (DS1) occurs, on average, for $IDR_1 = \alpha_1 \cdot IDR_{peak} = 0.30 \cdot IDR_{peak}$. For *Medium-Severe Damage* (DS2), the observed IDR value is equal, on average, to about $IDR_2 = \alpha_2 \cdot IDR_{peak} = 1.00 \cdot IDR_{peak}$ (α_2=0.92), that is, for hollow-clay masonry infills, in tune with the assumptions by Ricci et al. (2016), Sassun et al. (2016). Finally, for *Very Heavy Damage* (DS3) and *Collapse* (DS4) the values of α_3 and α_4 are equal to 2.50 and 4.50, respectively.

As a result, DS2 can be associated to the achievement of the in-plane maximum lateral strength of the infill panel. On the other hand, DS1 results to occur on the ascendant branch of the infill response and it corresponds, on average, to a lateral strength of 70% with respect to the peak load, thus coinciding to the (macro-) cracking point of the infill response (see Section 3). Finally, DS3 results associated to a mean strength reduction of 40% with respect to the peak load on the softening branch of in-plane behaviour, and DS4 is reached at 30% of the peak load on average, namely, generally before than the lateral strength contribution due to infill panel becomes totally null (being the latter an upper bound for the achievement of DS4).

In conclusion, the relationship shown in Eq. (4) could finally allow extending the IDR evaluation for each DS to the remaining 21 tests for which only the response of infill panel is available, as obtained and reported in Del Gaudio et al. (2017) and De Risi et al. (2018).

4.3 Influence of openings

The number of tests with openings is quite limited with respect to tests without openings, as shown in Section 2. However, the experimental campaigns dedicated to infills with openings generally analyse also the corresponding frame infilled with a solid panel, used as reference, being the same all the other variables. This peculiar condition – which unlikely occurs for other parameters affecting infill performance – makes possible the analysis of the influence of openings starting from each single experimental campaign, just comparing displacement capacity of such a "reference solid" panel and the corresponding infills with doors or windows openings. The ratios Ω between IDR capacity of each specimen with openings and its corresponding "reference solid" test are calculated. At DS1, the increment of displacement capacity appears systematic for each specimen with openings with respect to the "reference solid" test; at DS2, the ratio Ω varies between 0.90 and 1.38; more variability of Ω can be finally observed at DS3 and DS4 (Del Gaudio et al., 2018).

In summary, mean and CoV values of the Ω_i (i = 1,…,4) ratios are finally shown in Table 5. As a result, the increment of displacement capacity due to openings considering all DSs ($\overline{\Omega}$), weighted depending on the number of specimens for each DSs, is quite limited and in particular equal to +8%.

The coefficient $\overline{\Omega}$ commented above could be useful to modify fragility curves for infills with openings starting from fragility curves presented in Section 4.2. In particular, it can be assumed that, for all DSs, the IDR capacity values of infills without openings can be multiplied by the same coefficient, $\overline{\Omega}$, to obtain the IDR capacity of the corresponding infills with openings. As a result, $\overline{\Omega}$ can be adopted as a multiplier of the median drift capacity (e^{μ}) of fragility curves obtained in Section 4.2, being the same the logarithmic standard deviation.

Table 5. Ω ratios at each DS for infills with hollow clay bricks

Ω		DS1	DS2	DS3	DS4	$\overline{\Omega}$
	n_i	4	13	4	12	
Hollow Clay Bricks	**mean**	**1.11**	**1.03**	**0.87**	**1.19**	**1.08**
	CoV	0.08	0.14	0.21	0.30	

Note that the collected tests on masonry infills with openings are characterised by doors and windows with an opening percentages (void-to-total infill area) ranging between 10% and 40%. Opening eccentricity for the collected tests ranges between zero and 0.33, where the eccentricity is defined as the ratio between the horizontal distance between the mid-point of the opening length and the mid-point of the infill length (x) and the infill length itself (L_w). The opening size (l_{op}/L_w) - where l_{op} is the horizontal opening length – ranges between 25% and 50% (see De Risi et al. (2018) and Del Gaudio et al. (2018) for more details). Finally no ties or other steel reinforcement are present around the openings for all the collected tests.
Certainly, more data should be available for a more comprehensive analysis of the effect of openings on displacement capacity of masonry infill panels, also taking into account the opening size and its eccentricity. Nevertheless, to this aim, further experimental works should be performed in the future for the analysed masonry typology, since currently the amount of data is still quite small.

5. CONCLUSIONS

In this paper, a homogenous extensive database of experimental tests on RC frames infilled with hollow clay-masonry bricks – typical of Italian and Mediterranean RC building stock –is collected and presented.
For each test belonging to such a database, the experimental response of masonry infills under lateral loads have been obtained by means of the experimental responses of the infilled frames and the corresponding bare frames and their damage evolution is investigated in details.
The main and widely used nonlinear numerical models existing in literature for infills in the context of single-strut models have been investigated and compared with the experimental results in order to select the model that minimizes the prediction error. Furthermore, model by Panagiotakos and Fardis (1996) appears easier to apply, since it requires a very limited number of mechanical parameters to be defined, even if it is not able to predict a failure mode for the infill panel. Therefore, finally, a slight modification of the latter model has been proposed to significantly reduce the mean percentage errors in the prediction of the infill in-plane behaviour under lateral loads. The resulting infill envelope is a simple practice-oriented quadri-linear curve – which defines a single-strut representing the infill panel – that shows mean relative errors lower than 3% for all the parameters adopted to define the backbone curve. Further efforts should be certainly performed in future works to reduce the dispersion in the prediction.
On the other hand, thanks to the analysis of the evolutions of damage under increasing displacement demand for the collected tests, the displacement capacity at given performance levels have been also identified and correlated to in-plane behaviour of the infill panels. The definition of Damage States (DSs) is assumed according to the proposal by Cardone and Perrone (2015) and displacement capacity at each DS is evaluated. Empirical cumulative distribution functions have been obtained and lognormal fragility functions have been adopted to fit such data by using the Method of Maximum Likelihood. The evaluation of the influence of the presence of openings on the damage assessment of hollow clay brick panels, considering a quite limited number of test, has also been performed and presented. Windows or doors openings generally appeared to slightly increase the displacement

capacity of infill panels with hollow clay bricks.

ACKNOWLEDGMENTS

This work was developed under the support of ReLUIS-DPC 2014-2018 "*PR2. Strutture in cemento armato-WP6. Capacità sismica di tamponature ed interventi di rafforzamento"*, funded by the Italian Department of Civil Protection (DPC), and AXA Research Fund Post-Doctoral Grant "*Advanced nonlinear modelling and performance assessment of masonry infills in RC buildings under seismic loads: the way forward to design or retrofitting strategies and reduction of losses*". These supports are gratefully acknowledged.

REFERENCES

Baggio C., Bernardini A., Colozza R., Coppari S., Corazza L., Della Bella M., Di Pasquale G., Dolce M., Goretti A., Martinelli A., Orsini G., Papa F., Zuccaro G., (2007). Field manual for post-earthquake damage and safety assessment and short term countermeasures. Translation from Italian: Goretti A., Rota M., *JRC Scientific and Technical Reports*, EUR 22868 EN-2007.

Bergami A.V., and Nuti C. (2015). Experimental tests and global modeling of masonry infilled frames. *Earthquakes and Structures, 9*(2), 281-303.

Bertoldi, S. H., Decanini L. D., and Gavarini C. (1993). Telai tamponati soggetti ad azioni sismiche, un modello semplificato: confronto sperimentale e numerico. Proceedings of *6th Convegno Nazionale L'ingegneria sismica in Italia* (1993): 815-24. (in Italian)

Cardone D., and Perrone, G. (2015). Developing fragility curves and loss functions for masonry infill walls. *Earthquakes and Structures* 9.1 (2015): 257-279.

Chiozzi, A., and Miranda, E. (2017). Fragility functions for masonry infill walls with in□plane loading. *Earthquake Engineering & Structural Dynamics*, 46(15), 2831-2850.

Colangelo F. (2013). Drift-sensitive non-structural damage to masonry-infilled reinforced concrete frames designed to Eurocode 8. *Bulletin of Earthquake Engineering*, 11(6), 2151-2176.

De Risi M.T., Del Gaudio C., Ricci P., Verderame G.M. (2017). Simplified numerical modelling for hollow clay-masonry infills in RC frames under in-plane seismic loads, Proceedings of *ANIDIS 2017*, 17-21 September, Pistoia, Italy.

De Risi M.T., Del Gaudio C., Ricci P., Verderame G.M. (2018). In-plane behaviour and damage assessment of masonry infills with hollow clay bricks in RC frames. *Engineering Structures*, under review.

De Sortis A., Bazzurro P., Mollaioli F., Bruno S. (2007). Influenza delle tamponature sul rischio sismico degli edifici in calcestruzzo armato." Proc. of the *12th National Conference ANIDIS.*

Decreto Ministeriale del 14/1/2008. Approvazione delle nuove norme tecniche per le costruzioni. G.U. n. 29 del 4/2/2008 (in Italian)

Del Gaudio C., De Risi M.T., Ricci P., Verderame G.M. (2017). Fragility functions for clay masonry infills in RC buildings under in-plane seismic actions, Proceedings of *ANIDIS 2017*, 17-21 September, Pistoia, Italy.

Del Gaudio C., De Risi M.T., Ricci P., Verderame G.M. (2018). Seismic damage assessment and loss estimation due to infills in reinforced concrete frames. *Bulletin of Earthquake Engineering*, under review

Dolšek, M., and Fajfar, P. (2008). The effect of masonry infills on the seismic response of a four-storey reinforced concrete frame—a deterministic assessment. *Engineering Structures*, 30(7), 1991-2001.

Drysdale RG, Hamid AA. Tensile strength of brick masonry. International Journal of Masonry Construction 1982; 2 (4):172–177.

Fardis MN, Panagiotakos TB (1997) Seismic design and response of bare and masonry-infilled reinforced concrete buildings. Part II: infilled structures. *J Earthq Eng* 1(3):475–503

FEMA (Federal Emergency Management Agency), (1998). FEMA 306 Evaluation of earthquake damaged concrete and masonry wall buildings. Washington, D.C.

FEMA (Federal Emergency Management Agency), (2000). FEMA 356, Prestandard and Commentary for the Seismic Rehabilitation of Buildings. Washington, D.C.

FEMA P-58, ATC - Applied Technology Council (2012b), FEMA P-58 Next-generation Seismic Performance Assessment for Buildings, Volume 2 - Implementation Guide, Federal Emergency Management Agency, Washington, DC.

Hak S., Morandi P., Magenes G. (2013). Evaluation of infill strut properties based on in-plane cyclic tests. *Građevinar* 65 (2013) 6, 509-521.

Jeon, J. S., Park, J. H., & DesRoches, R. (2015). Seismic fragility of lightly reinforced concrete frames with masonry infills. Earthquake Engineering & Structural Dynamics, 44(11), 1783-1803.

Lowes L. (2009). FEMA P-58/BD-3.8.6- Background Document. Fragility Functions for Reinforced Concrete Moment Frames.

Mainstone RJ (1971). On the stiffnesses and strengths of infilled frames. *Proc Inst Civil Eng* (Suppl 4): 57–90

Panagiotakos T.B., and Fardis M.N., (1996). Seismic response of infilled RC frames structures. Proceedings of the *11th World Conference on Earthquake Engineering*, Acapulco, México. Paper No. 225.

Pires, F. and Carvalho, E.C. (1992). The behaviour of infilled reinforced concrete frames under horizontal cyclic loading. Proceedings of the *10th World Conference on Earthquake Engineering*, Madrid.

Ricci, P., De Risi, M. T., Verderame, G. M., & Manfredi, G. (2013). Influence of infill distribution and design typology on seismic performance of low-and mid-rise RC buildings. *Bulletin of Earthquake Engineering*, 11(5), 1585-1616.

Ross, S.M. (2003), Peirce's criterion for the elimination of suspect experimental data, *J. Eng. Technol.*, 20(2), 38-41.

Stylianidis, K. C. (1988). Cyclic Behaviour of infilled R/C frames. *Brick and Block Masonry (8 th IBMAC)* London, Elsevier Applied Science, 2, 792-799.

Verderame G.M., Ricci P., Del Gaudio C., De Risi M.T. (2016). Experimental tests on masonry infilled gravity- and seismic-load designed RC frames, Brick and Block Masonry: Trends, Innovations and Challenges - Proceedings of the *16th International Brick and Block Masonry Conference, IBMAC 2016*, pp. 1349-1358